ISSN 2307-8960 (online)

World Journal of *Clinical Cases*

World J Clin Cases 2023 February 6; 11(4): 719-978

Published by Baishideng Publishing Group Inc

World Journal of Clinical Cases

Contents

Thrice Monthly Volume 11 Number 4 February 6, 2023

MINIREVIEWS

719 Development and refinement of diagnostic and therapeutic strategies for managing patients with cardiogenic stroke: An arduous journey

Fan ZX, Liu RX, Liu GZ

725 Portal vein aneurysm-etiology, multimodal imaging and current management

Kurtcehajic A, Zerem E, Alibegovic E, Kunosic S, Hujdurovic A, Fejzic JA

ORIGINAL ARTICLE

Clinical and Translational Research

738 CD93 serves as a potential biomarker of gastric cancer and correlates with the tumor microenvironment

Li Z, Zhang XJ, Sun CY, Fei H, Li ZF, Zhao DB

Retrospective Study

756 Chest computed tomography findings of the Omicron variants of SARS-CoV-2 with different cycle threshold values

Ying WF, Chen Q, Jiang ZK, Hao DG, Zhang Y, Han Q

764 Major depressive disorders in patients with inflammatory bowel disease and rheumatoid arthritis

Haider MB, Basida B, Kaur J

780 Selective laser trabeculoplasty as adjunctive treatment for open-angle glaucoma *vs* following incisional glaucoma surgery in Chinese eyes

Zhu J, Guo J

788 Efficacy of transvaginal ultrasound-guided local injections of absolute ethanol for ectopic pregnancies with intrauterine implantation sites

Kakinuma T, Kakinuma K, Matsuda Y, Yanagida K, Ohwada M, Kaijima H

Clinical Trials Study

797 Efficacy of incremental loads of cow's milk as a treatment for lactose malabsorption in Japan

Hasegawa M, Okada K, Nagata S, Sugihara S

Observational Study

809 Transdiagnostic considerations of mental health for the post-COVID era: Lessons from the first surge of the pandemic

Goldstein Ferber S, Shoval G, Rossi R, Trezza V, Di Lorenzo G, Zalsman G, Weller A, Mann JJ

821 Effect of patient COVID-19 vaccine hesitancy on hospital care team perceptions

Caspi I, Freund O, Pines O, Elkana O, Ablin JN, Bornstein G

World Journal of Clinical Cases

Thrice Monthly Volume 11 Number 4 February 6, 2023

Contents

Randomized Clinical Trial

830 Improvement of inflammatory response and gastrointestinal function in perioperative of cholelithiasis by Modified Xiao-Cheng-Qi decoction

Sun BF, Zhang F, Chen QP, Wei Q, Zhu WT, Ji HB, Zhang XY

CASE REPORT

844 Metagenomic next-generation sequencing for pleural effusions induced by viral pleurisy: A case report

Liu XP, Mao CX, Wang GS, Zhang MZ

852 *Clostridium perfringens* gas gangrene caused by closed abdominal injury: A case report and review of the literature

Li HY, Wang ZX, Wang JC, Zhang XD

859 Is lymphatic invasion of microrectal neuroendocrine tumors an incidental event?: A case report

Ran JX, Xu LB, Chen WW, Yang HY, Weng Y, Peng YM

866 *Pneumocystis jirovecii* diagnosed by next-generation sequencing of bronchoscopic alveolar lavage fluid: A case report and review of literature

Cheng QW, Shen HL, Dong ZH, Zhang QQ, Wang YF, Yan J, Wang YS, Zhang NG

874 Identification of 1q21.1 microduplication in a family: A case report

Huang TT, Xu HF, Wang SY, Lin WX, Tung YH, Khan KU, Zhang HH, Guo H, Zheng G, Zhang G

883 Double pigtail catheter reduction for seriously displaced intravenous infusion port catheter: A case report

Liu Y, Du DM

888 Thyroid storm in a pregnant woman with COVID-19 infection: A case report and review of literatures

Kim HE, Yang J, Park JE, Baek JC, Jo HC

896 Computed tomography diagnosed left ovarian venous thrombophlebitis after vaginal delivery: A case report

Wang JJ, Hui CC, Ji YD, Xu W

903 Preoperative 3D reconstruction and fluorescent indocyanine green for laparoscopic duodenum preserving pancreatic head resection: A case report

Li XL, Gong LS

909 Unusual presentation of systemic lupus erythematosus as hemophagocytic lymphohistiocytosis in a female patient: A case report

Peng LY, Liu JB, Zuo HJ, Shen GF

918 Polyarteritis nodosa presenting as leg pain with resolution of positron emission tomography-images: A case report

Kang JH, Kim J

922 Easily misdiagnosed complex Klippel-Trenaunay syndrome: A case report

Li LL, Xie R, Li FQ, Huang C, Tuo BG, Wu HC

World Journal of Clinical Cases

Thrice Monthly Volume 11 Number 4 February 6, 2023

Contents

931 Benign lymphoepithelial cyst of parotid gland without human immunodeficiency virus infection: A case report

Liao Y, Li YJ, Hu XW, Wen R, Wang P

938 Epithelioid trophoblastic tumor of the lower uterine segment and cervical canal: A case report

Yuan LQ, Hao T, Pan GY, Guo H, Li DP, Liu NF

945 Treatment of portosystemic shunt-borne hepatic encephalopathy in a 97-year-old woman using balloon-occluded retrograde transvenous obliteration: A case report

Nishi A, Kenzaka T, Sogi M, Nakaminato S, Suzuki T

952 Development of Henoch-Schoenlein purpura in a child with idiopathic hypereosinophilia syndrome with multiple thrombotic onset: A case report

Xu YY, Huang XB, Wang YG, Zheng LY, Li M, Dai Y, Zhao S

962 Three cases of jejunal tumors detected by standard upper gastrointestinal endoscopy: A case series

Lee J, Kim S, Kim D, Lee S, Ryu K

972 Omental infarction diagnosed by computed tomography, missed with ultrasonography: A case report

Hwang JK, Cho YJ, Kang BS, Min KW, Cho YS, Kim YJ, Lee KS

World Journal of Clinical Cases

Thrice Monthly Volume 11 Number 4 February 6, 2023

Contents

ABOUT COVER

Editorial Board Member of *World Journal of Clinical Cases*, Sahand Samieirad, DDS, MS, MSc, Associate Professor, Oral and Maxillofacial Surgery Department, Mashhad Dental School, Mashhad University of Medical Sciences, Mashhad 9178613111, Iran. samieerads@mums.ac.ir

AIMS AND SCOPE

The primary aim of *World Journal of Clinical Cases* (*WJCC*, *World J Clin Cases*) is to provide scholars and readers from various fields of clinical medicine with a platform to publish high-quality clinical research articles and communicate their research findings online.

WJCC mainly publishes articles reporting research results and findings obtained in the field of clinical medicine and covering a wide range of topics, including case control studies, retrospective cohort studies, retrospective studies, clinical trials studies, observational studies, prospective studies, randomized controlled trials, randomized clinical trials, systematic reviews, meta-analysis, and case reports.

INDEXING/ABSTRACTING

The *WJCC* is now abstracted and indexed in Science Citation Index Expanded (SCIE, also known as SciSearch®), Journal Citation Reports/Science Edition, Current Contents®/Clinical Medicine, PubMed, PubMed Central, Scopus, Reference Citation Analysis, China National Knowledge Infrastructure, China Science and Technology Journal Database, and Superstar Journals Database. The 2022 Edition of Journal Citation Reports® cites the 2021 impact factor (IF) for *WJCC* as 1.534; IF without journal self cites: 1.491; 5-year IF: 1.599; Journal Citation Indicator: 0.28; Ranking: 135 among 172 journals in medicine, general and internal; and Quartile category: Q4. The *WJCC*'s CiteScore for 2021 is 1.2 and Scopus CiteScore rank 2021: General Medicine is 443/826.

RESPONSIBLE EDITORS FOR THIS ISSUE

NAME OF JOURNAL
World Journal of Clinical Cases

ISSN
ISSN 2307-8960 (online)

LAUNCH DATE
April 16, 2013

FREQUENCY
Thrice Monthly

PUBLICATION DATE
February 6, 2023

World Journal of Clinical Cases

Submit a Manuscript: https://www.f6publishing.com

World J Clin Cases 2023 February 6; 11(4): 738-755

DOI: 10.12998/wjcc.v11.i4.738

ISSN 2307-8960 (online)

ORIGINAL ARTICLE

Clinical and Translational Research

CD93 serves as a potential biomarker of gastric cancer and correlates with the tumor microenvironment

Zheng Li, Xiao-Jie Zhang, Chong-Yuan Sun, He Fei, Ze-Feng Li, Dong-Bing Zhao

Specialty type: Gastroenterology and hepatology

Provenance and peer review: Unsolicited article; Externally peer reviewed.

Peer-review model: Single blind

Peer-review report's scientific quality classification

Grade A (Excellent): A
Grade B (Very good): B
Grade C (Good): 0
Grade D (Fair): 0
Grade E (Poor): 0

P-Reviewer: Dilek ON, Turkey; Koganti SB, United States

Received: October 12, 2022
Peer-review started: October 12, 2022
First decision: December 13, 2022
Revised: December 13, 2022
Accepted: January 3, 2023
Article in press: January 3, 2023
Published online: February 6, 2023

Zheng Li, Xiao-Jie Zhang, Chong-Yuan Sun, He Fei, Ze-Feng Li, Dong-Bing Zhao, Department of Pancreatic and Gastric Surgical Oncology, National Cancer Center/National Clinical Research for Cancer/Cancer Hospital, Chinese Academy of Medical Sciences and Peking Union Medical College, Beijing 100021, China

Corresponding author: Dong-Bing Zhao, MD, Professor, Department of Pancreatic and Gastric Surgical Oncology, National Cancer Center/National Clinical Research for Cancer/Cancer Hospital, Chinese Academy of Medical Sciences and Peking Union Medical College, No. 17 Pan-Jia-Yuan South Lane, Chaoyang District, Beijing 100021, China. dbzhao@cicams.ac.cn

Abstract

BACKGROUND

The tumor microenvironment (TME) plays an important role in the growth and expansion of gastric cancer (GC). Studies have identified that CD93 is involved in abnormal tumor angiogenesis, which may be related to the regulation of the TME.

AIM

To determine the role of CD93 in GC.

METHODS

Transcriptomic data of GC was investigated in a cohort from The Cancer Genome Atlas. Additionally, RNA-seq data sets from Gene Expression Omnibus (GSE118916, GSE52138, GSE79973, GSE19826, and GSE84433) were applied to validate the results. We performed the immune infiltration analyses using ESTIMATE, CIBERSORT, and ssGSEA. Furthermore, weighted gene co-expression network analysis (WGCNA) was conducted to identify the immune-related genes.

RESULTS

Compared to normal tissues, CD93 significantly enriched in tumor tissues (t = 4.669, 95%CI: 0.342-0.863, P < 0.001). Higher expression of CD93 was significantly associated with shorter overall survival (hazard ratio = 1.62, 95%CI: 1.09-2.4, P = 0.017), less proportion of CD8 T and activated natural killer cells in the TME (P < 0.05), and lower tumor mutation burden (t = 4.131, 95%CI: 0.721-0.256, P < 0.001). Genes co-expressed with CD93 were mainly enriched in angiogenesis. Moreover, 11 genes were identified with a strong relationship between CD93 and the immune microenvironment using WGCNA.

CONCLUSION
CD93 is a novel prognostic and diagnostic biomarker for GC, that is closely related to the immune infiltration in the TME. Although this retrospective study was a comprehensive analysis, the prospective cohort studies are preferred to further confirm these conclusions.

Key Words: Gastric cancer; CD93; Tumor microenvironment; Immunotherapy; Prognosis; Biomarker

Core Tip: Gastric cancer (GC) is an aggressive malignancy, with a 5-year survival rate lower than 20%. The disease burden caused by GC remains heavy worldwide. In this study, various analyses were performed using transcriptomic profiles from the Gene Expression Omnibus databases and The Cancer Genome Atlas. Finally, enrichment analysis and protein-protein interaction network were constructed. CD93 is identified as a diagnostic and prognostic biomarker of GC, which is closely related to the immune infiltration in the tumor microenvironment. Then, Immune-related gene modules were identified to further reveal the relationship between CD93 and immune characteristics.

Citation: Li Z, Zhang XJ, Sun CY, Fei H, Li ZF, Zhao DB. CD93 serves as a potential biomarker of gastric cancer and correlates with the tumor microenvironment. *World J Clin Cases* 2023; 11(4): 738-755
URL: https://www.wjgnet.com/2307-8960/full/v11/i4/738.htm
DOI: https://dx.doi.org/10.12998/wjcc.v11.i4.738

INTRODUCTION

As a common malignancy of the digestive tract tumor, gastric cancer (GC) is the fourth leading cause of cancer-related mortality worldwide, and the 5-year survival rate of GC is lower than 20%[1]. Treatments for GC include endoscopic resection, surgery (D2 lymphadenectomy), perioperative or adjuvant chemotherapy, targeted therapy, immunotherapy, and so on. Among them, immunotherapy for GC has attracted more attention in recent years[2,3]. The tumor microenvironment (TME) refers to tumor cells and their surrounding cellular matrix, including blood vessels, and immune cells, and is an important factor influencing the effect of immunotherapy on GC[4]. Targeting and suppressing the immunosuppressive properties of the TME can enhance the overall response rate (ORR) to immunotherapy, including immune checkpoint inhibitors (ICIs)[5-7]. CD93 is known as a C1q receptor that is involved in a variety of biological processes, such as the inflammatory response, tumor angiogenesis, matrix regulation, and innate lymphoid cell function [8-10], which suggests that CD93 may participate in the regulation of the TME. A recent study has found that blocking the CD93 pathway contributes to drug transport and immunotherapy efficacy by normalizing the vasculature of tumors. CD93 pathway blockade can improve the efficacy of chemotherapy and immunotherapy[11]. Although the roleof CD93 in some tumors has been explored, the specific role of CD93 in GC is still unclear.

Given these considerations, we were deeply interested in the relationship between CD93 and immune infiltration in the TME and the value of CD93 in the diagnosis, prognosis, and immunotherapy of GC. Therefore, the RNA-seq transcriptome profiles of stomach adenocarcinoma (STAD) within The Cancer Genome Atlas (TCGA) and Gene Expression Omnibus (GEO) were investigated. We first performed a pan-cancer analysis to identify the general significance of CD93 in cancers. Then, we divided patients with GC in this study into two groups according to the expression of CD93, and we compared the groups in terms of immune cell infiltration, gene mutation landscape, tumor mutational burden, and so on.

MATERIALS AND METHODS

Data sources and processing

Gene expression RNA-seq (HTSeq-Counts, HTSeq-FPKM) and survival data in a cohort of TCGA Stomach Cancer were downloaded from UCSC Xena[12]. HTSeq-FPKM of 375 tumor samples and 32 normal samples were used for further analysis. HTSeq-Counts data were used to identify the differential expressed genes (DEGs) of low and high CD93 expression groups using the R package DESeq2 [13] (|log2FoldChange| > 1 and adjusted $P < 0.05$). Expression profiling data in 5 datasets (GSE118916, GSE52138, GSE79973, GSE19826, and GSE84433) from GEO[14] were downloaded as validation sets.

Mutation data (MuTect2) including 414 patients with STAD from TCGA were processed using R package maftools[15]. The waterfall plot was used to show the genetic mutation using the R package ComplexHeatmap[16].

Pan-cancer analysis

To understand the general significance of CD93 in cancers, we compared the expression levels of CD93 between tumor tissues and normal tissues in various cancer types using TIMER2.0[17]. Additionally, TISIDB[18] was also used to obtain the relationship between CD93 expression and the OS of these cancer types.

Diagnostic and prognostic value analysis

We compared CD93 expression levels of GC and normal tissues in both unpaired and paired samples and visualize outcomes using R package ggplot2. Receiver operating characteristic (ROC) curves and Kaplan-Meier survival analysis were conducted to further explore the diagnostic and prognostic value of CD93, and R packages pROC[19] and survminer were used for visualization, respectively. Univariate and multivariate COX proportional hazards models were established for better understanding. In addition, Immunohistochemistry and Immunofluorescence of CD93 were obtained from Human Protein Atlas[20].

Functional enrichment analysis

Genes that were significantly positively or negatively related to CD93 were identified using LinkedOmics[21]. Heatmaps were used to show the top 50 positively and the top 50 negatively correlated genes. Then, we constructed a protein-protein interaction (PPI) network of positively correlated genes *via* GeneMANIA[22]. Gene Ontology (GO) and Kyoto Encyclopedia of Genes and Genomes (KEGG) enrichment analyses of these genes were performed using the R package clusterProfiler[23].

Immune infiltration analysis

A plot from the TIMER[24] was used to show the correlations between the CD93 expression level and B cell, CD8+T Cell, CD4+T cell, macrophage, neutrophil, and dendritic cell. ESTIMATE is a method to identify the proportions of stromal and immune cells, which can bring the in-depth exploration of TME. We evaluated the immune score (immune component), stromal score (stromal component), and ESTIMATE score (comprehensive score of immunity and matrix) of each sample from TCGA and GEO using the R package estimate[25]. CIBERSORT[26] is a tool to characterize the cell composition of various tissues. We calculate the proportion of 22 immune cells in each sample with STAD using this method. Then, we conducted the ssGSEA to evaluate the infiltration level of 28 immune cell types based on the published immune gene sets[27] using the R package GSVA[28].

Weighted gene co-expression network analysis

Weighted gene co-expression network analysis (WGCNA) was applied to identify the module genes related to CD93 and the immunity of patients with STAD using the R package WGCNA[29] (softPower = 4). Nine modules were obtained to calculate their relationships with stromal score, immune score, ESTIMATE score, and tumor purity. Finally, we identified 11 hub genes based on the value of module membership (MM) > 0.80 and gene significance (GS) > 0.85.

Analysis of hub genes

The PPI network and GO enrichment analysis of 11 hub genes were performed using the R package clusterProfiler and STRING[30], respectively. Then, we calculated Spearman's correlation of 11 hub genes, hub gene-ESTIMATE, and hub gene-ssGSEA using the R package corrplot.

Statistical analysis

All statistical analyses mentioned in this article were conducted by R (version 4.2.0) and SPSS (version 25.0). Weltch't test and Spearman's coefficient were used for box plots and correlation analysis, respectively. We evaluated statistical significance using two-sided t-tests and defined it as $^{a}P < 0.05$, $^{b}P < 0.01$, and $^{c}P < 0.001$.

RESULTS

Pan-cancer analysis of CD93

The expression of CD93 between tumor and normal tissues in various cancers was compared using TIMER2.0, suggesting that CD93 expression was significantly different between tumor and normal tissues in various types of cancers ($P < 0.05$) (Figure 1A). We further investigated the effect of CD93 on OS across human cancers *via* the TISIDB. It showed that high CD93 expression led to shorter overall

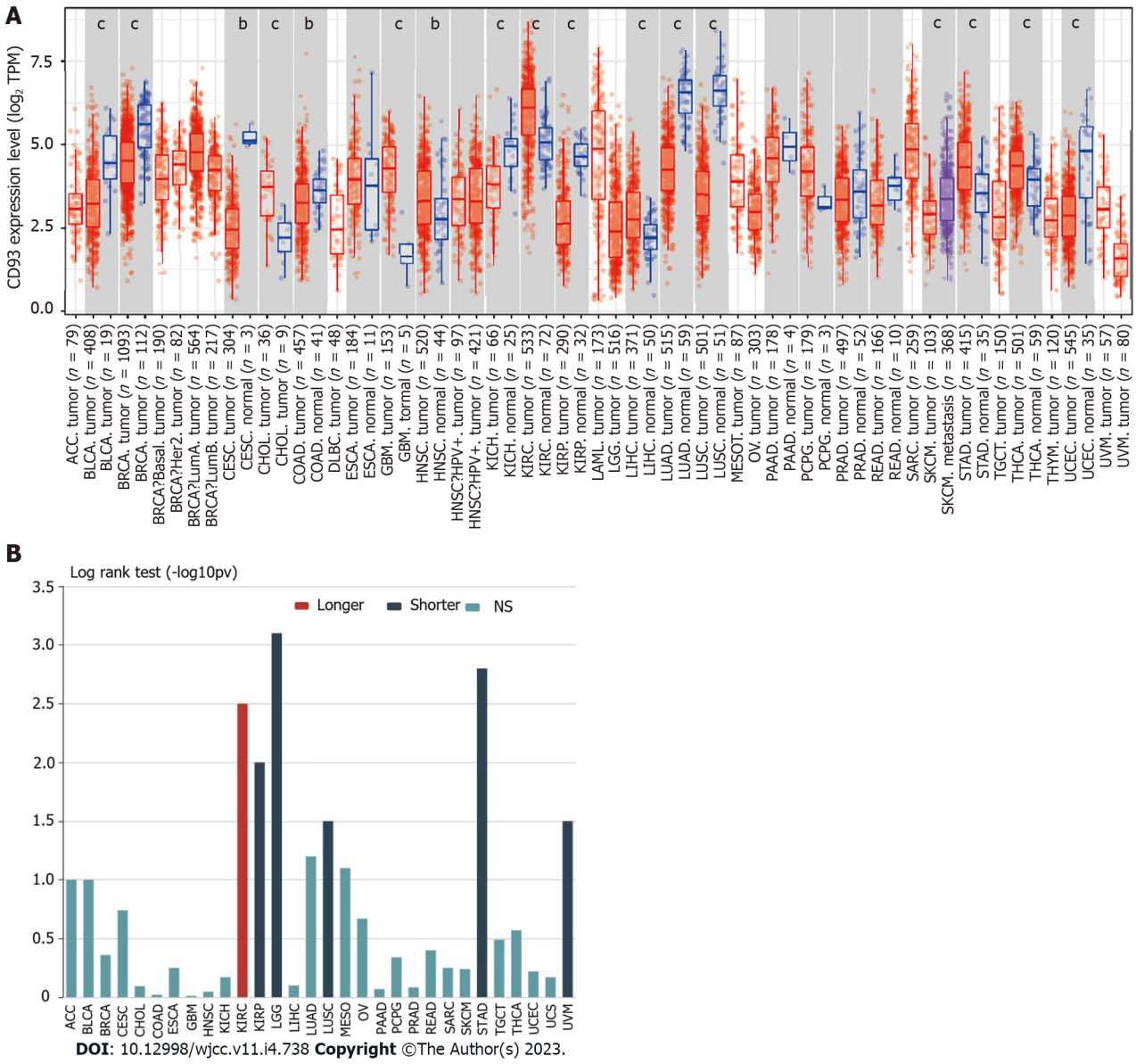

Figure 1 Pan-cancer analysis of CD93. A: Differential expression of CD93 between normal and tumor tissues in pan-cancer based on the TIMER2.0; B: Associations between CD93 expression and overall survival in pan-cancer. The *P* values are labeled as $^{a}P < 0.05$, $^{b}P < 0.01$, $^{c}P < 0.001$.

survival in STAD, kidney renal papillary cell carcinoma, brain lower-grade glioma, lung squamous cell carcinoma, and uveal melanoma, while leading to a longer one in kidney renal clear cell carcinoma (Figure 1B).

Diagnostic value for GC of CD93

The CD93 expression levels of unpaired and paired samples from TCGA were both significantly higher in GC than in normal tissues ($t = 4.669$, 95%CI: 0.342-0.863, $P < 0.001$; $t = 3.238$, 95%CI: 0.196-0.877, $P = 0.003$) (Figure 2A and B). In addition, expression data obtained from GEO (GSE118916, GSE52138, GSE79973, and GSE19826) was applied for verification (Figure 2H-K). All datasets from TCGA and GEO showed a significantly higher expression of CD93 in GC tissues than in normal tissues ($P < 0.05$). Immunohistochemistry indicated higher CD93 expression in GC tissues than in normal tissues from the protein level (Figure 2E). Immunofluorescence indicated that CD93 mainly expressed in vesicles, plasma membrane, and toggle channels (Figure 2F). Furthermore, ROC curves were performed using the datasets mentioned above to evaluate the diagnostic value of CD93, the area under the curve was 0.695, 0.876, 0.806, 0.750, and 0.771, respectively (Figure 2C and L-O).

Prognostic value for GC of CD93

Samples from the TCGA STAD dataset were divided into two groups by the CD93 expression level, including the low CD93 expression group (low, $n = 114$) and the high CD93 expression group (high, $n = 220$). Kaplan-Meier analysis of two groups was conducted, suggesting that patients with high

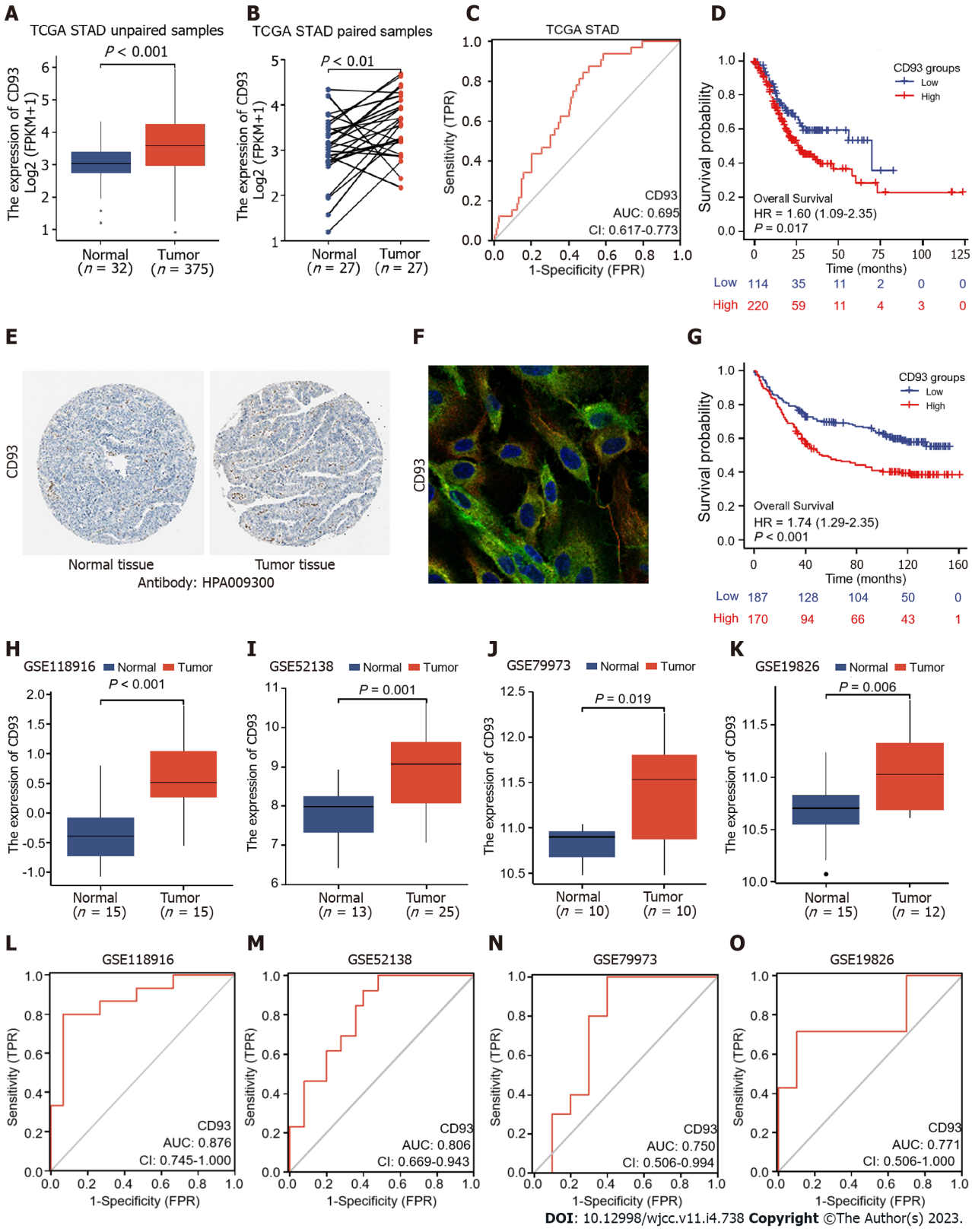

DOI: 10.12998/wjcc.v11.i4.738

Figure 2 Diagnostic and prognostic value analysis. A and B: Differential expression of CD93 between gastric cancer (GC) and normal tissues in unpaired samples (A), paired samples (B); C: Receiver operating characteristic (ROC) curve of overall survival based on CD93 in The Cancer Genome Atlas stomach adenocarcinoma; D: Kaplan-Meier analysis of OS between two groups; E: Immunohistochemistry of CD93 between GC and normal tissues; F: Immunofluorescence of CD93; H-K: Differential expression of CD93 in 4 validation datasets (GSE118916, GSE52138, GSE79973, and GSE19826); L-O: ROC curves of 4 validation datasets based on CD93.

expression of CD93 had significantly shorter OS [hazard ratio (HR) = 1.60, 95%CI: 1.09-2.35, P = 0.017] (Figure 2D). In addition, we set GSE84433 with 357 GC patients as an external independent validation dataset and divided these patients into low-CD93 (low, n = 178) and high-CD93 (high, n = 179)

Table 1 Univariate and multivariate Cox regression analysis of overall survival

Characteristics	Univariate analysis			Multivariate analysis		
	HR	95%CI	*P* value	HR	95%CI	*P* value
Age	1.02	1.01-1.04	0.002	1.03	1.02-1.05	< 0.001
Grade						
G1	Reference					
G2	2.64	0.36-19.18	0.337			
G3	3.53	0.49-25.38	0.209			
G4	3.54	0.37-34.07	0.274			
Gender	1.31	0.91-1.9	0.145			
Stage						
I	Reference			Reference		
II	1.45	0.75-2.8	0.268	1.41	0.73-2.74	0.307
III	2.11	1.14-3.91	0.018	1.99	1.07-3.71	0.03
IV	3.65	1.81-7.39	< 0.001	4.97	2.41-10.22	< 0.001
CD93 (high *vs* low)	1.6	1.09-2.35	0.017	1.62	1.09-2.4	0.017

HR: Hazard ratio.

expression groups. A similar result could be drawn from the Kaplan–Meier analysis that patients in the high-CD93 expression group had a shorter OS (HR: 1.74, 95%CI: 1.29-2.35, $P < 0.001$) (Figure 2G). Univariate and multivariate COX regression analysis were conducted as Table 1, indicating CD93 was a significant independent prognostic risk factor for GC (HR = 1.62, 95%CI: 1.09-2.40, $P = 0.017$). The baseline patient characteristics were summarized in Table 2.

Identification and enrichment analysis of correlation genes

Correlation analysis with CD93 based on the Pearson test was conducted using LinkedOmics. The result was visualized by a volcano plot (Figure 3A). We obtained 7026 significantly positively correlated genes (red dots) and 5308 significantly negatively ones (green dots), respectively. In addition, we showed heatmaps of the top 50 positively correlated and the top 50 negatively correlated genes (Figure 3B and C). PPI network of the top 10 positive CD93 co-expressed genes was further constructed using GeneMANIA, suggesting functions of "angiogenesis", "endothelium development", and "regulation of angiogenesis" (Figure 3D). GO enrichment analysis of positive CD93 co-expressed genes mainly enriched in "ameboidal-type cell migration" (biological process), "collagen-containing extracellular matrix" (cell component), and "growth factor binding" (molecular function) (Figure 3E). KEGG pathway enrichment analysis indicated that these genes mainly participated in the "PI3K-Akt signaling pathway", "Focal adhesion", and "Pathways in cancer" (Figure 3F).

Immune-related analysis in the TME

The expression of CD93 was positively proportional to CD8+T Cell, CD4+T cell, macrophage, neutrophil, and dendritic cell ($P < 0.05$) (Figure 4A). Furthermore, CD93 expression tended to have a positive correlation with ESTIMATE results (immune score, stromal score, and ESTIMATE score) ($P < 0.05$) (Figure 4B-D). Then, we performed the CIBERSORT for determining the proportion of 22 immune cells in each sample with STAD (Figure 4E). The proportion of 22 immune cells in two groups was compared using CIBERSORT, suggesting the proportion of CD8 T cells, follicular helper T cells, and activated NK cells in the high CD93 expression group was significantly lower than that in the low CD93 expression group, whereas Monocytes, Dendritic cells resting, and Mast cells resting had just the reverse ($P < 0.05$) (Figure 4F). ssGSEA showed that 24 types of immune cell (such as activated B cell, activated CD8 T cell, activated dendritic cell, central memory CD4 T cell, and central memory CD8 T cell) had a significantly higher expression in the high CD93 expression group, while CD56 bright natural killer (NK) cell had a lower expression in this group ($P < 0.05$) (Figure 4G).

Gene mutation analysis and tumor mutation burden comparison

Gene mutation of GC is closely related to its therapeutic efficacy. Accordingly, a waterfall plot was used to identify the top 15 significant gene mutations (such as *TTN*, *MUC16*, and *LRP1B*) between two groups ($P < 0.05$) (Figure 5A). Furthermore, we made a comparison of tumor mutation burden (TMB) between

Table 2 Baseline patient characteristics

Characteristics	high-CD93 (*n* = 220)	low-CD93 (*n* = 114)	Overall (*n* = 334)
Age, yr (mean ± SD)	64.8 ± 12.8	64.1 ± 10.3	64.5 ± 12.0
Gender, *n* (%)			
Female	72 (32.7)	48 (42.1)	120 (35.9)
Male	148 (67.3)	66 (57.9)	214 (64.1)
Grade, *n* (%)			
G1	4 (1.8)	4 (3.5)	8 (2.4)
G2	66 (30.0)	50 (43.9)	116 (34.7)
G3	143 (65.0)	59 (51.8)	202 (60.5)
GX	7 (3.2)	1 (0.9)	8 (2.4)
pT, *n* (%)			
T1	5 (2.3)	10 (8.8)	15 (4.5)
T2	45 (20.5)	25 (21.9)	70 (21.0)
T3	103 (46.8)	53 (46.5)	156 (46.7)
T4	67 (30.5)	26 (22.8)	93 (27.8)
pN, *n* (%)			
N0	63 (28.6)	40 (35.1)	103 (30.8)
N1	62 (28.2)	24 (21.1)	86 (25.7)
N2	43 (19.5)	26 (22.8)	69 (20.7)
N3	48 (21.8)	22 (19.3)	70 (21.0)
NX	4 (1.8)	2 (1.8)	6 (1.8)
pM, *n* (%)			
M0	194 (88.2)	105 (92.1)	299 (89.5)
M1	17 (7.7)	4 (3.5)	21 (6.3)
MX	9 (4.1)	5 (4.4)	14 (4.2)
Stage, *n* (%)			
Stage I	24 (10.9)	22 (19.3)	46 (13.8)
Stage II	75 (34.1)	35 (30.7)	110 (32.9)
Stage III	96 (43.6)	48 (42.1)	144 (43.1)
Stage IV	25 (11.4)	9 (7.9)	34 (10.2)

low and high CD93 expression groups, which indicated that patients with high CD93 expression had a lower TMB (t = 4.131, 95%CI: 0.721-0.256, P < 0.001) (Figure 5B). The mutation rate of CD93 in GC ranked fourth in pan-cancer (Figure 5C).

Identification of hub genes in the immune microenvironment of GC

A total of 1679 DEGs (966 upregulated and 713 downregulated) were obtained between low and high CD93 expression groups. Then, we visualize the results using a volcano plot (Figure 6A). WGCNA was conducted to identify a module related to CD93 expression and immune infiltration (Figure 6B-D). The Yellow module was screened out because of its high correlation with immunity (r = 0.89, $P = 5 \times 10^{-122}$), hence we acquired 11 hub genes (*MPEG1*, *IL10RA*, *SRGN*, *SLA*, *DOCK2*, *NCKAP1L*, *IKZF1*, *PTPRC*, *SIGLEC10*, *PLEK*, *P2RY10*) from the yellow module based on MM > 0.80 and GS > 0.85 (Figure 6E).

Analysis of 11 hub genes

GO enrichment analysis identified these genes were mainly enriched in "positive regulation of phagocytosis" (biological process), "cytoplasmic side of plasma membrane" (cell component), and "interleukin-10 binding" (molecular function) (Figure 7A). Furthermore, we constructed a PPI network and made a correlation analysis of these genes (Figure 7B and C). Correlation analysis between these

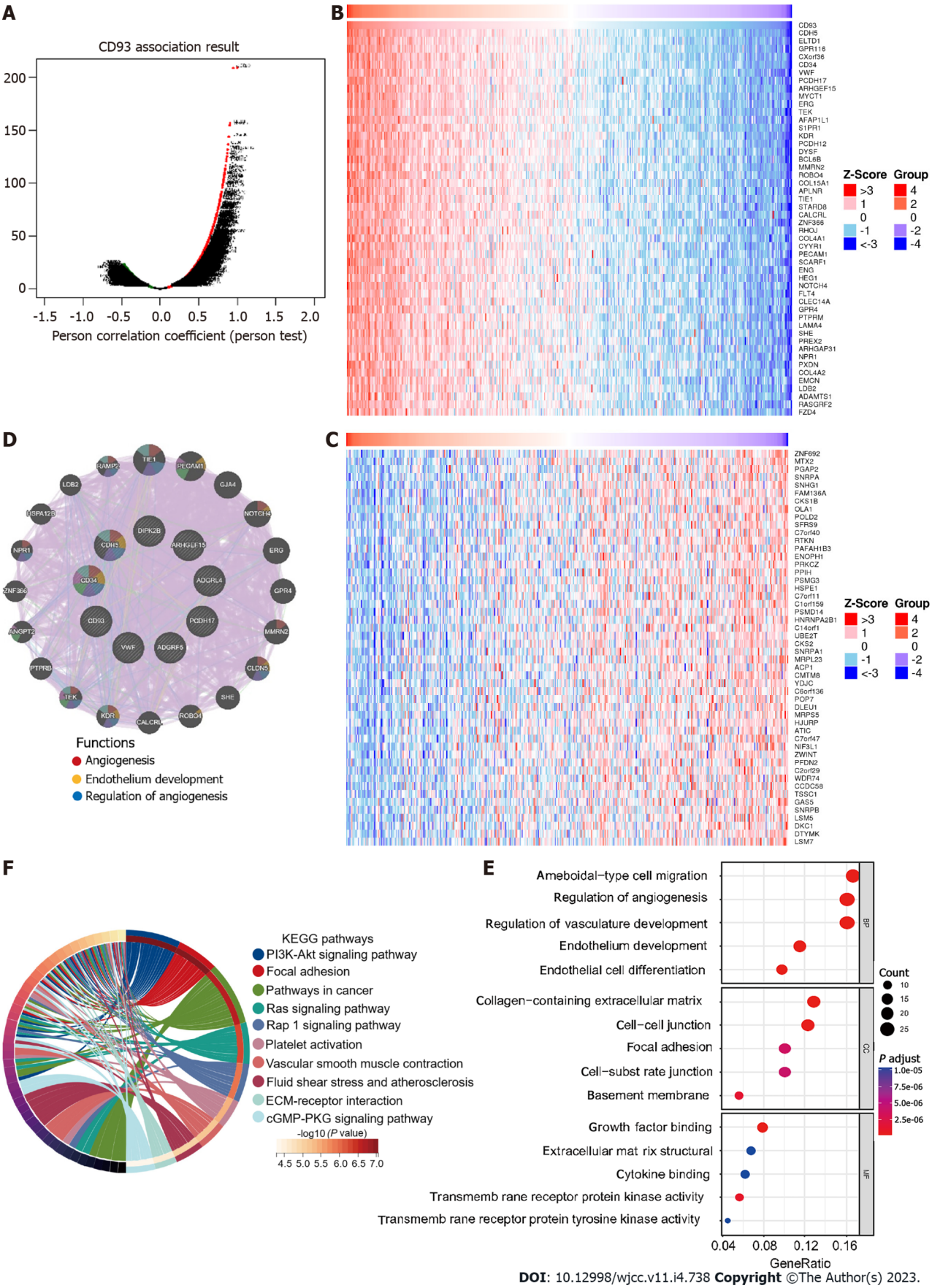

DOI: 10.12998/wjcc.v11.i4.738

Figure 3 Function and pathway analysis. A: Genes are highly correlated with CD93; B: Heatmap of the top 50 positive correlation genes; C: Heatmap of the top 50 negative correlation genes; D: Protein-protein interaction of the top positive correlation genes; E: The Gene Ontology enrichment analysis; F: The Kyoto Encyclopedia of Genes and Genomes pathways enrichment analysis.

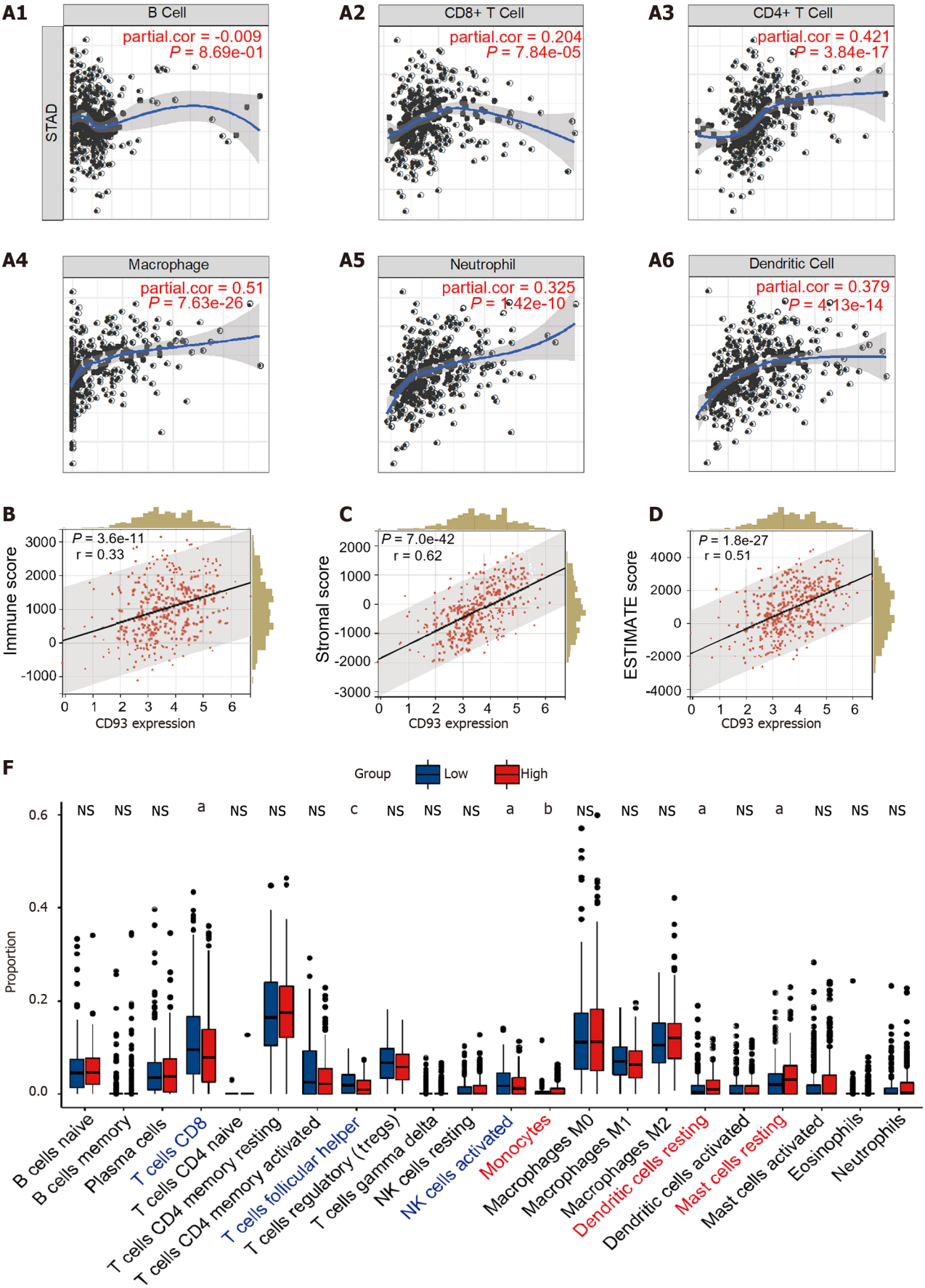
A1
B Cell
STAD
partial.cor = -0.009
P = 8.69e-01
A2
CD8+ T Cell
partial.cor = 0.204
P = 7.84e-05
A3
CD4+ T Cell
partial.cor = 0.421
P = 3.84e-17
A4
Macrophage
partial.cor = 0.51
P = 7.63e-26
A5
Neutrophil
partial.cor = 0.325
P = 1.42e-10
A6
Dendritic Cell
partial.cor = 0.379
P = 4.13e-14
B
P = 3.6e-11
r = 0.33
Immune score
CD93 expression
C
P = 7.0e-42
r = 0.62
Stromal score
CD93 expression
D
P = 1.8e-27
r = 0.51
ESTIMATE score
CD93 expression
F
Group
Low
High
Proportion
B cells naive
B cells memory
Plasma cells
T cells CD8
T cells CD4 naive
T cells CD4 memory resting
T cells CD4 memory activated
T cells follicular helper
T cells regulatory (tregs)
T cells gamma delta
NK cells resting
NK cells activated
Monocytes
Macrophages M0
Macrophages M1
Macrophages M2
Dendritic cells resting
Dendritic cells activated
Mast cells resting
Mast cells activated
Eosinophils
Neutrophils

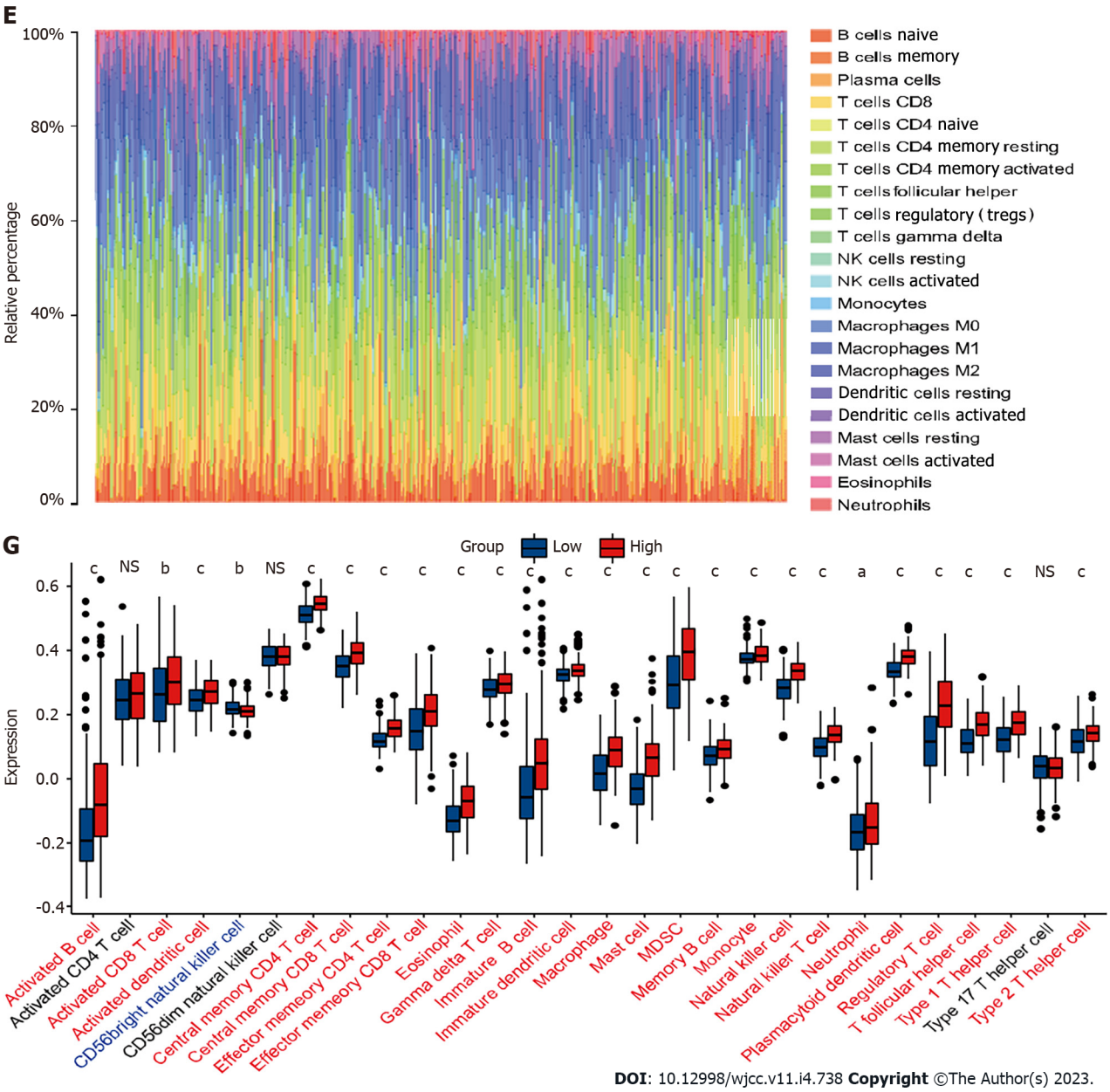

DOI: 10.12998/wjcc.v11.i4.738

Figure 4 Immune characteristics in tumor microenvironment. A: Correlation between CD93 and six types of immune cells based on TIMER; B-D: Correlation between CD93 and immune score (B), stromal score (C), ESTIMATE score (D); E: The proportion of immune cell infiltration; F: Different proportions of immune cells infiltration between two groups; G: Expression of immune cells between two groups *via* ssGSEA. The *P* values are labeled as $^{a}P < 0.05$, $^{b}P < 0.01$, $^{c}P < 0.001$, NS: No significance.

genes and TME (ESTIMATE and ssGSEA) suggested that these genes were closely related to both stromal components and immune infiltration in GC (Figure 7D and E).

Validation of immune-related characteristics in TME

GSE84433 (357 samples) was set as an external independent validation dataset. We performed ESTIMATE, CIBERSORT, and ssGSEA to evaluate the immune-related characteristics of CD93 in TME again. Then, several similar results as before could be obtained. CD93 expression was positively correlated with the ESTIMATE results (Figure 8A-C). CIBERSORT showed the proportion of various immune cell types in each sample (Figure 8D). The proportion of follicular helper T cells and activated NK cells in the high-CD93 expression group was lower compared to that in the low-CD93 expression group (Figure 8E). ssGSEA indicated that 24 immune cell types (including activated B cell, activated CD8 T cell, and activated dendritic cell) expressed significantly higher in the high-CD93 expression group (Figure 8F). Accordingly, CD93 was identified to be closely related to immune infiltration in TME of GC.

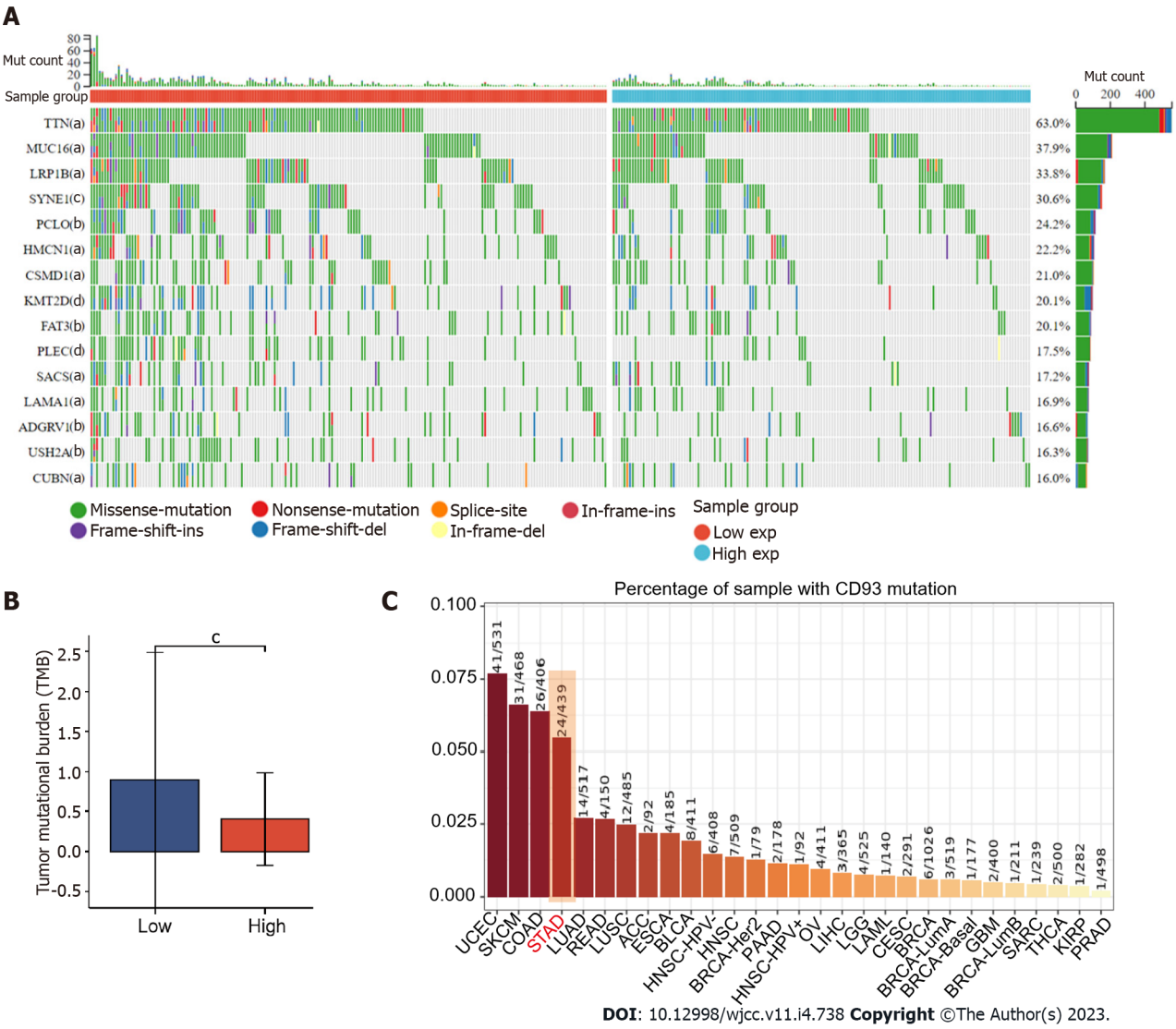

DOI: 10.12998/wjcc.v11.i4.738

Figure 5 Gene mutation and tumor mutational burden comparison. A: Comparison of mutational landscapes between two groups; B: Comparison of tumor mutational burden between two groups; C: The mutation rate of CD93 in gastric cancer ranked fourth in pan-cancer. The *P* values are labeled as $^{a}P < 0.05$, $^{b}P < 0.01$, $^{c}P < 0.001$.

DISCUSSION

In this study, we applied bioinformatics technology to determine the specific role of CD93 in GC. Various analytical methods identified that CD93 is a biomarker for the diagnosis and prognosis of GC. Concerning the potential mechanisms of CD93, enrichment analysis was performed. Consistent with previous studies[11], CD93 was found to be involved in the formation of tumor blood vessels in GC. Such disordered, immature, and impermeable blood vessels can lead to poor tumor blood perfusion. The resulting hypoxic microenvironment can promote the production of more aggressive tumor cells and limit the killing effect of immune cells[31]. In addition to regulating angiogenesis, GO enrichment analysis suggested that CD93 is involved in matrix formation including cell junction, focal adhesion, and regulation of cytokine production, which further demonstrates the important status of CD93 in TME. Also worth noting is that CD93 plays a critical role in the PI3K-Akt signaling pathway. The PI3K-Akt pathway is constantly found to be activated in various cancers and has been considered a promising target for therapy. Multiple activators of this pathway have been proved to possess oncogenic potentials *in vivo* and *in vitro* with diverse mechanisms, including stimulation of metabolic reprogramming, proliferation, and so on[32]. These tend to be part of the reasons for the poor prognosis of patients with GC induced by CD93.

As important components of the TME, immune cells can inhibit or promote tumor progression by interacting with tumor cells[33]. The investigation of immune components in TME brings a deeper understanding of the biological characteristics, prognosis, and other information of tumors. Based on ESTIMATE, CIBERSORT, and ssGSEA, a comparison of immune cell infiltration between low and high CD93 expression groups was conducted. According to the result of ESTIMATE, we found that CD93

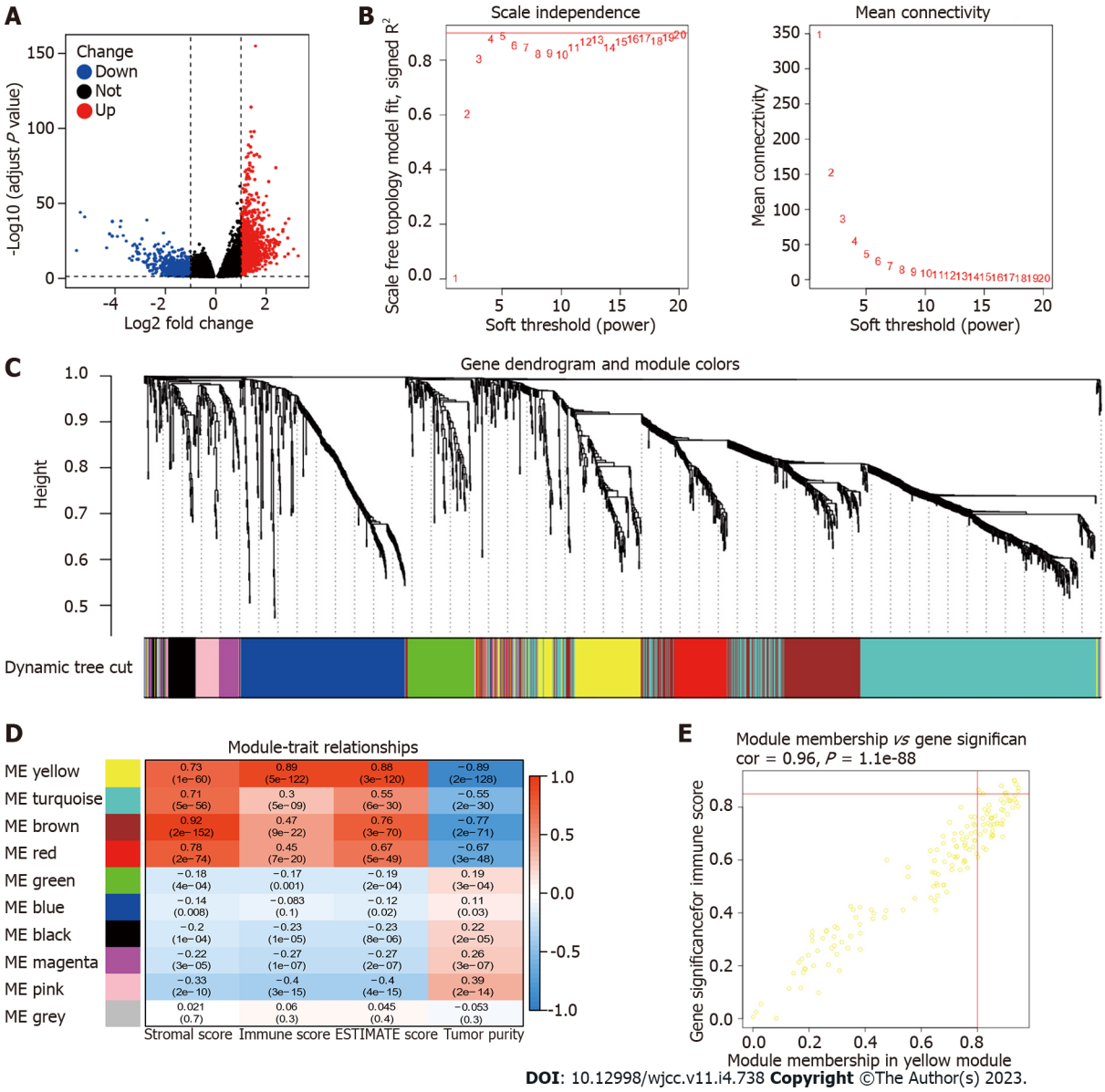

DOI: 10.12998/wjcc.v11.i4.738 **Copyright** ©The Author(s) 2023.

Figure 6 Identification of the key genes related to CD93 in the tumor immune microenvironment. A: Volcano plot of variance analysis; B: Analysis of network topology for soft powers; C: Gene dendrogram and module colors; D: Heatmap between modules and ESTIMATE results; E: Scatter plot of genes in the yellow module.

was significantly proportional to immunity. Previous studies could give reasonable explanations for this result. The blood vessel wall mainly consists of endothelial cells, pericytes, and smooth muscle cells. On the one hand, these cells can activate T cells by expressing MHCI, MHCII, and some costimulatory factors such as CD80, and CD86 to participate in the immune response[34]. On the other hand, a variety of immune cell subsets, including NK cells, T helper 17 cells, regulatory T lymphocytes, and functional subsets of macrophages can act as regulators of arteriogenesis[35]. The crosstalk between the vascular system and immunity explains the high correlation between CD93 and immunity.

From the proportion of immune cell expression, CD8 T cells, Follicular helper T cells, and activated NK cells showed a lower proportion in the high CD93 expression group, while monocytes, resting dendritic cells, and resting mast cells had just the reverse. This is probably caused by local microenvironment hypoxia and accumulation of metabolic end-products induced by abnormal vascular proliferation due to high expression of CD93. CD8 T cells and NK cells are important effector cells involved in anti-tumor immune response in TME and are related to tumor progression and prognosis[36,37]. At present, CD8 T cells have been described as a variety of subtypes, including Tc1, Tc2, Tc9, Tc17, and Tc22, each with different cytotoxicity and effects. Among these cell subtypes, Tc17 and Tc22 are the main T cell subtypes in gastric tissue. Tc17 has no cytotoxicity, and its high expression is negatively correlated with the survival time of GC, while Tc22 is just the opposite. Besides, follicular helper T cells are the key to the production of germinal center formation[38]. They interact with tumor-specific B cells to enhance the anti-tumor effect of CD8 T cells. In summary, the reduced proportion of these important

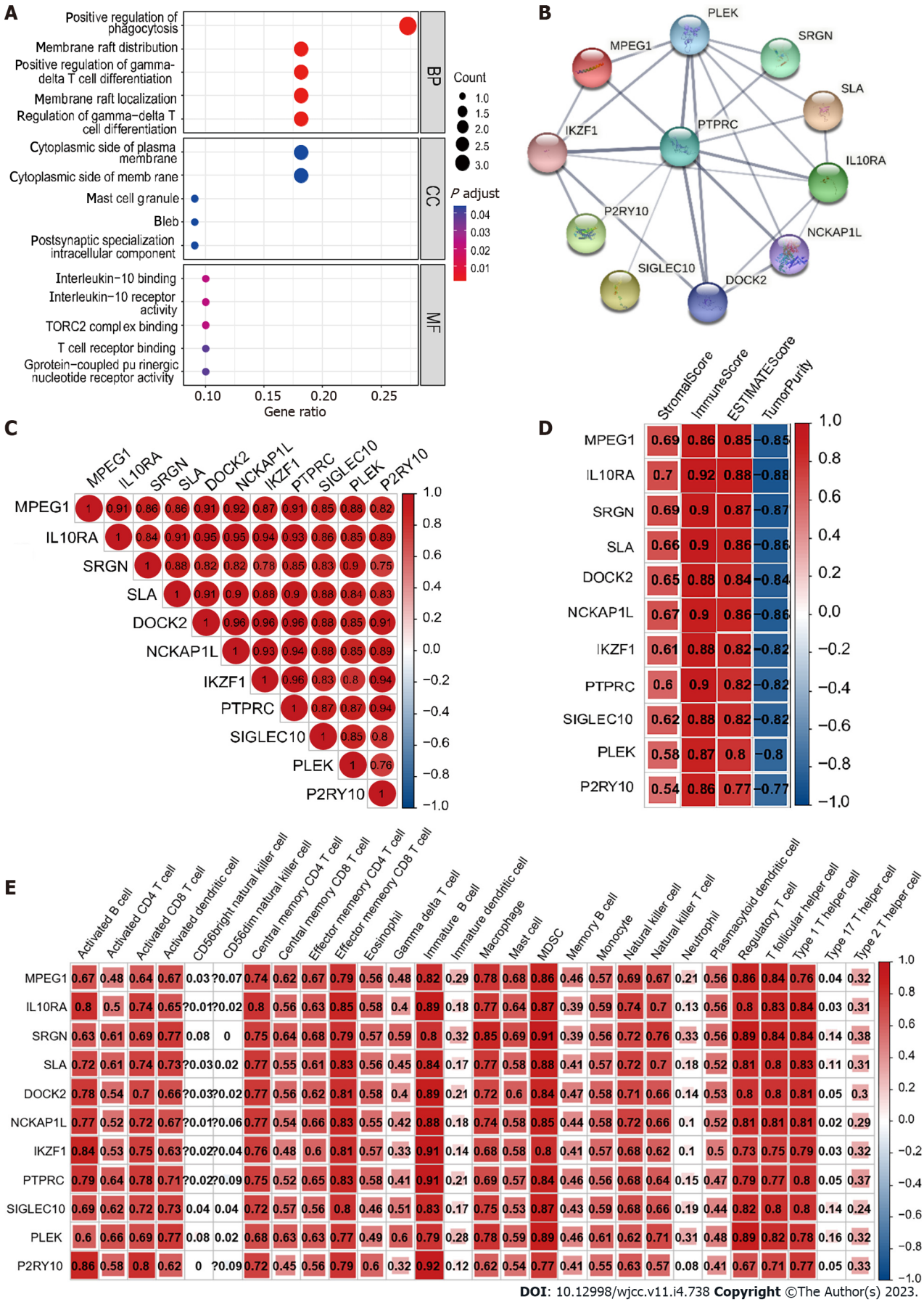

DOI: 10.12998/wjcc.v11.i4.738

Figure 7 Analysis of 11 hub genes. A: The Gene Ontology analysis of hub genes; B: Protein-protein interaction network of hub genes; C: Relevance between hub genes; D: Correlation between hub genes and ESTIMATE results; E: Correlation between hub genes and expression of immune cells.

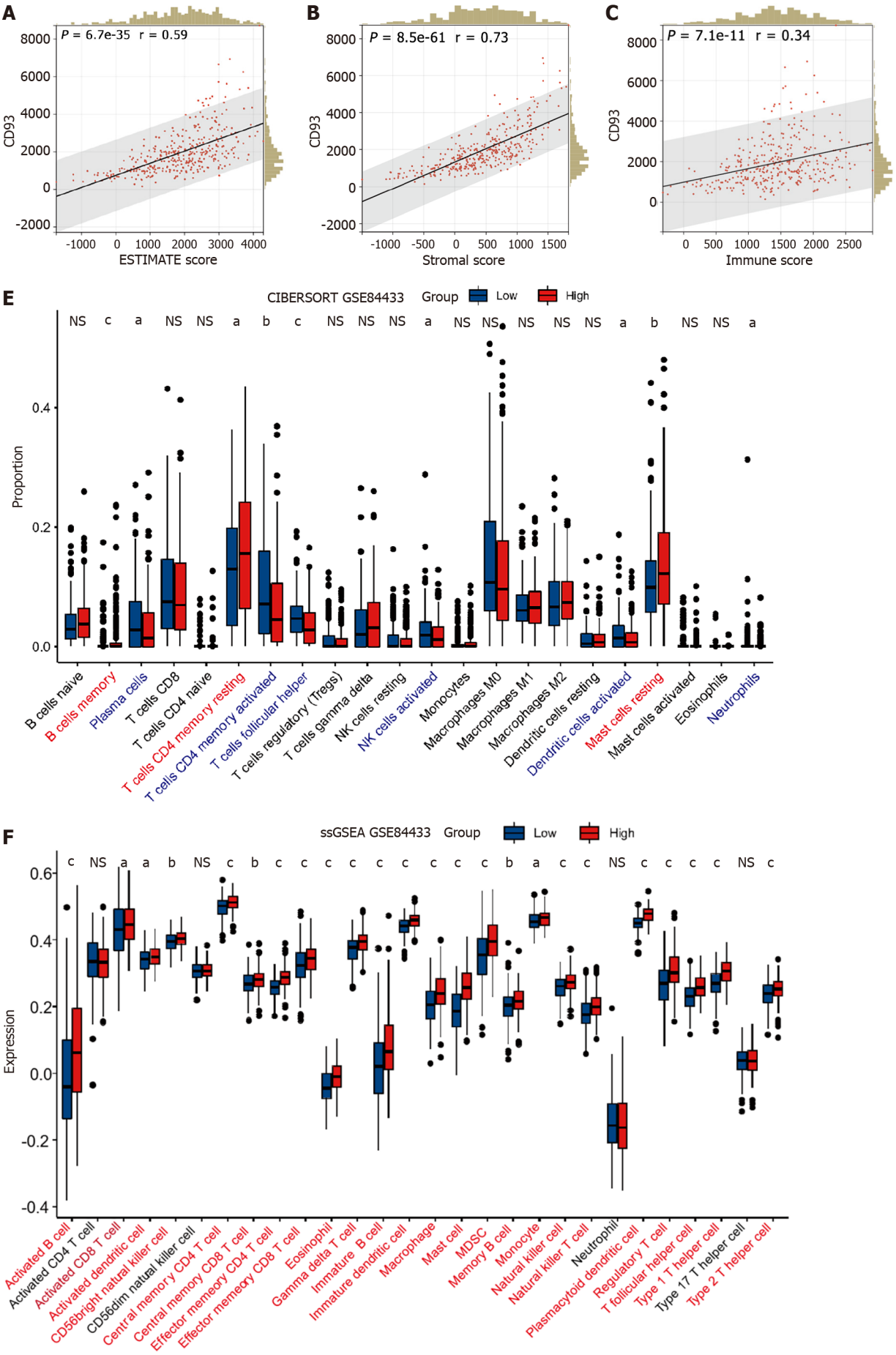
A
P = 6.7e-35 r = 0.59
CD93
ESTIMATE score
B
P = 8.5e-61 r = 0.73
CD93
Stromal score
C
P = 7.1e-11 r = 0.34
CD93
Immune score
E
CIBERSORT GSE84433 Group Low High
Proportion
B cells naive
B cells memory
Plasma cells
T cells CD8
T cells CD4 naive
T cells CD4 memory resting
T cells CD4 memory activated
T cells follicular helper
T cells regulatory (Tregs)
T cells gamma delta
NK cells resting
NK cells activated
Monocytes
Macrophages M0
Macrophages M1
Macrophages M2
Dendritic cells resting
Dendritic cells activated
Mast cells resting
Mast cells activated
Eosinophils
Neutrophils
F
ssGSEA GSE84433 Group Low High
Expression
Activated B cell
Activated CD4 T cell
Activated CD8 T cell
Activated dendritic cell
CD56bright natural killer cell
CD56dim natural killer cell
Central memory CD4 T cell
Central memory CD8 T cell
Effector memeory CD4 T cell
Effector memeory CD8 T cell
Eosinophil
Gamma delta T cell
Immature B cell
Immature dendritic cell
Macrophage
Mast cell
MDSC
Memory B cell
Monocyte
Natural killer cell
Natural killer T cell
Neutrophil
Plasmacytoid dendritic cell
Regulatory T cell
T follicular helper cell
Type 1 T helper cell
Type 17 T helper cell
Type 2 T helper cell

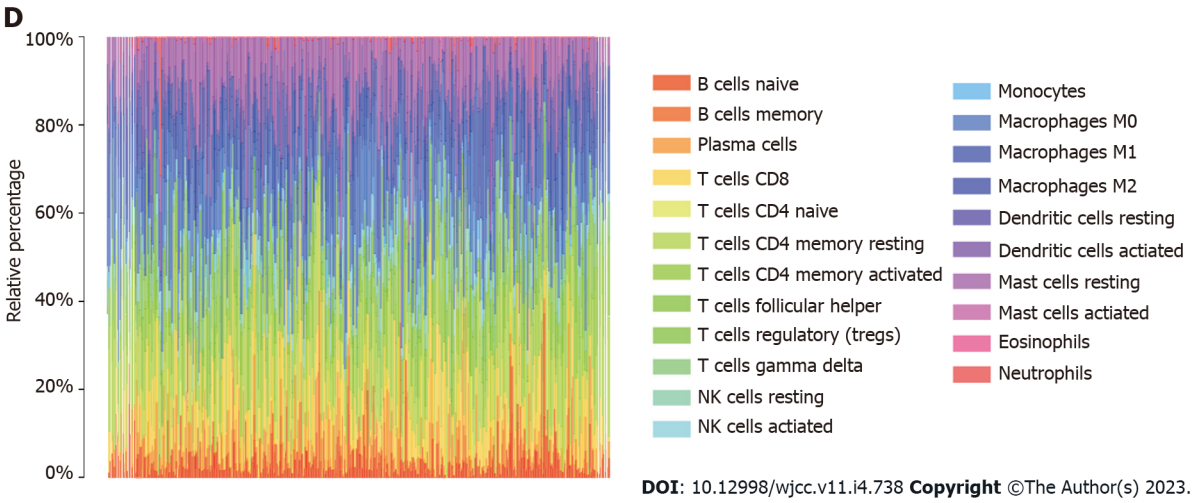

DOI: 10.12998/wjcc.v11.i4.738

Figure 8 Validation of immune characteristics. A-C: Correlation between CD93 and ESTIMATE score (A), stromal score (B), immune score (C). D: Cibersort; E: Different proportions of immune cells infiltration between two groups; F: ssGSEA. The *P* values are labeled as $^{a}P < 0.05$, $^{b}P < 0.01$, $^{c}P < 0.001$, NS: No significance.

immune cells in the TME may be the main reason for the poor prognosis caused by CD93. However, analysis of the expression of immune cells in two groups suggested that various types of immune cells were highly expressed in the high CD93 expression group. Although blood vessels are conducive to tissue growth and immune response, they can contribute to inflammation and malignant diseases. Abnormal angiogenesis induced by CD93 in TME can promote tumor growth and form an immune-hostile microenvironment[39], and this effect exceeds its immune enhancement effect, which makes the prognosis of the high CD93 expression group with high immune infiltration still poor.

In recent years, the ICIs represented by PD-1, PD-L1, and CTLA-4 bring considerable disease relief to tumor patients, playing an important role in tumor immunotherapy. However, not all patients can benefit from ICIs. A series of studies have shown that TMB is a potential biomarker for predicting the response to ICIs and patients with high TMB possess a better immunotherapeutic effect of ICIs[40,41]. In this study, we made a comparison of gene mutational landscape and TMB between two groups. The results showed that GC patients with high expression of CD93 had a lower TMB, indicating that the effect of immunotherapy in GC patients with high expression of CD93 is poor. Then, we performed WGCNA to identify the key genes related to CD93 in the tumor immune microenvironment of GC. We obtained 11 genes from the yellow module. Among them, SRGN overexpression has been previously shown to promote colorectal cancer metastasis and predict a poor prognosis of hepatocellular carcinoma [42,43]. This time, the identification of these 11 genes can help us further understand the immune microenvironment of GC and suggest potential methods for immunotherapy of GC in the future.

Although we have taken a variety of methods to obtain a comprehensive understanding of the relationship between CD93 and GC, we use 5 cohorts (GSE118916, GSE52138, GSE79973, GSE19826, and GSE84433) as external validation sets, some limitations of this study should be recognized. First, this is a retrospective study. Selection bias, loss of follow-up bias, recall bias, and other biases exist in the study. Thus, a prospective study is required to avoid these biases. Furthermore, limited by TCGA and GEO, we only performed research and analysis from the genetic level. A study that can demonstrate CD93 expression from the protein level or reveal the direct mechanism needs to be conducted in the future.

CONCLUSION

All in all, comprehensive analyses were applied using transcriptomic profiles and survival information from the GEO and TCGA databases, suggesting that CD93 is a biomarker of diagnosis and prognosis for GC, which closely correlates with immune infiltration in TME. These data help us further comprehend the role of CD93 in the immune microenvironment and may suggest potential strategies for immunotherapy of GC in the future.

ARTICLE HIGHLIGHTS

Research background

Gastric cancer (GC) is a common malignancy with poor 5-year survival rate. Tumor microenvironment (TME) containing intricate interaction between immune and non-immune cells produces significant impact of the survival of GC. Additionally, CD93 was proved to be associated with abnormal angiogenesis, which could be involved in TME of GC.

Research motivation

This study was conducted to determine the specific role of CD93 in GC in order to provide insights for the discovery of novel therapeutic target of GC in the feature.

Research objectives

Cohorts data of GC patients was investigated from The Cancer Genome Atlas and Gene Expression Omnibus (GSE118916, GSE52138, GSE79973, GSE19826, and GSE84433).

Research methods

We performed a series of immune infiltration analyses using ESTIMATE, CIBERSORT, and ssGSEA. Furthermore, weighted gene co-expression network analysis was conducted to identify the immune-related genes.

Research results

CD93 significantly enriched in tumor tissues. Additionally, higher expression of CD93 was significantly associated with shorter overall survival, less proportion of CD8 T and activated nature killer cells in the TME, and lower tumor mutational burden.

Research conclusions

CD93 is a novel prognostic and diagnostic biomarker for GC, which is closely related to the immune infiltration in TME.

Research perspectives

CD93 can serve as a potential therapeutic target for the immunotherapy of GC in the feature.

FOOTNOTES

Author contributions: Li Z and Zhang XJ contributed to the conceptualization; Li Z contributed to the methodology; Sun CY contributed to the software; Li Z and Zhang XJ contributed to the validation; Li Z and Fei H contributed to the formal analysis; Li ZF contributed to the investigation; Zhao DB contributed to the resources; Li Z and Sun CY contributed to the writing-original draft preparation; All authors contributed to the writing-review and editing; Zhao DB contributed to the project administration. All authors have reviewed and agreed to the published version of the manuscript.

Conflict-of-interest statement: All authors declare no conflict of interest.

Data sharing statement: All data analyzed in this study can be available in XENA (http://xena.ucsc.edu), GEO (https://www.ncbi.nlm.nih.gov/geo/).

Country/Territory of origin: China

ORCID number: Zheng Li 0000-0003-4415-6552; Xiao-Jie Zhang 0000-0001-9850-9806; Chong-Yuan Sun 0000-0003-1354-2063; He Fei 0000-0003-4831-4028; Ze-Feng Li 0000-0002-5345-3527; Dong-Bing Zhao 0000-0002-6770-2694.

S-Editor: Zhang H
L-Editor: A
P-Editor: Zhang H

REFERENCES

1 **Sung H**, Ferlay J, Siegel RL, Laversanne M, Soerjomataram I, Jemal A, Bray F. Global Cancer Statistics 2020: GLOBOCAN Estimates of Incidence and Mortality Worldwide for 36 Cancers in 185 Countries. *CA Cancer J Clin* 2021; **71**: 209-249 [PMID: 33538338 DOI: 10.3322/caac.21660]

2 **Smyth EC**, Nilsson M, Grabsch HI, van Grieken NC, Lordick F. Gastric cancer. *Lancet* 2020; **396**: 635-648 [PMID: 32861308 DOI: 10.1016/S0140-6736(20)31288-5]

3 **Zhao Q**, Cao L, Guan L, Bie L, Wang S, Xie B, Chen X, Shen X, Cao F. Immunotherapy for gastric cancer: dilemmas and prospect. *Brief Funct Genomics* 2019; **18**: 107-112 [PMID: 30388190 DOI: 10.1093/bfgp/ely019]

4 **Rojas A**, Araya P, Gonzalez I, Morales E. Gastric Tumor Microenvironment. *Adv Exp Med Biol* 2020; **1226**: 23-35 [PMID: 32030673 DOI: 10.1007/978-3-030-36214-0_2]

5 **Kim J**, Hong J, Lee J, Fakhraei Lahiji S, Kim YH. Recent advances in tumor microenvironment-targeted nanomedicine delivery approaches to overcome limitations of immune checkpoint blockade-based immunotherapy. *J Control Release* 2021; **332**: 109-126 [PMID: 33571549 DOI: 10.1016/j.jconrel.2021.02.002]

6 **Xiao Y**, Yu D. Tumor microenvironment as a therapeutic target in cancer. *Pharmacol Ther* 2021; **221**: 107753 [PMID: 33259885 DOI: 10.1016/j.pharmthera.2020.107753]

7 **Lei Q**, Wang D, Sun K, Wang L, Zhang Y. Resistance Mechanisms of Anti-PD1/PDL1 Therapy in Solid Tumors. *Front Cell Dev Biol* 2020; **8**: 672 [PMID: 32793604 DOI: 10.3389/fcell.2020.00672]

8 **Lugano R**, Vemuri K, Yu D, Bergqvist M, Smits A, Essand M, Johansson S, Dejana E, Dimberg A. CD93 promotes β1 integrin activation and fibronectin fibrillogenesis during tumor angiogenesis. *J Clin Invest* 2018; **128**: 3280-3297 [PMID: 29763414 DOI: 10.1172/JCI97459]

9 **Huang J**, Lee HY, Zhao X, Han J, Su Y, Sun Q, Shao J, Ge J, Zhao Y, Bai X, He Y, Wang X, Dong C. Interleukin-17D regulates group 3 innate lymphoid cell function through its receptor CD93. *Immunity* 2021; **54**: 673-686.e4 [PMID: 33852831 DOI: 10.1016/j.immuni.2021.03.018]

10 **Nativel B**, Ramin-Mangata S, Mevizou R, Figuester A, Andries J, Iwema T, Ikewaki N, Gasque P, Viranaïcken W. CD93 is a cell surface lectin receptor involved in the control of the inflammatory response stimulated by exogenous DNA. *Immunology* 2019; **158**: 85-93 [PMID: 31335975 DOI: 10.1111/imm.13100]

11 **Sun Y**, Chen W, Torphy RJ, Yao S, Zhu G, Lin R, Lugano R, Miller EN, Fujiwara Y, Bian L, Zheng L, Anand S, Gao F, Zhang W, Ferrara SE, Goodspeed AE, Dimberg A, Wang XJ, Edil BH, Barnett CC, Schulick RD, Chen L, Zhu Y. Blockade of the CD93 pathway normalizes tumor vasculature to facilitate drug delivery and immunotherapy. *Sci Transl Med* 2021; **13** [PMID: 34321321 DOI: 10.1126/scitranslmed.abc8922]

12 **Goldman MJ**, Craft B, Hastie M, Repečka K, McDade F, Kamath A, Banerjee A, Luo Y, Rogers D, Brooks AN, Zhu J, Haussler D. Visualizing and interpreting cancer genomics data *via* the Xena platform. *Nat Biotechnol* 2020; **38**: 675-678 [PMID: 32444850 DOI: 10.1038/s41587-020-0546-8]

13 **Love MI**, Huber W, Anders S. Moderated estimation of fold change and dispersion for RNA-seq data with DESeq2. *Genome Biol* 2014; **15**: 550 [PMID: 25516281 DOI: 10.1186/s13059-014-0550-8]

14 **Barrett T**, Wilhite SE, Ledoux P, Evangelista C, Kim IF, Tomashevsky M, Marshall KA, Phillippy KH, Sherman PM, Holko M, Yefanov A, Lee H, Zhang N, Robertson CL, Serova N, Davis S, Soboleva A. NCBI GEO: archive for functional genomics data sets--update. *Nucleic Acids Res* 2013; **41**: D991-D995 [PMID: 23193258 DOI: 10.1093/nar/gks1193]

15 **Mayakonda A**, Lin DC, Assenov Y, Plass C, Koeffler HP. Maftools: efficient and comprehensive analysis of somatic variants in cancer. *Genome Res* 2018; **28**: 1747-1756 [PMID: 30341162 DOI: 10.1101/gr.239244.118]

16 **Gu Z**, Eils R, Schlesner M. Complex heatmaps reveal patterns and correlations in multidimensional genomic data. *Bioinformatics* 2016; **32**: 2847-2849 [PMID: 27207943 DOI: 10.1093/bioinformatics/btw313]

17 **Li T**, Fu J, Zeng Z, Cohen D, Li J, Chen Q, Li B, Liu XS. TIMER2.0 for analysis of tumor-infiltrating immune cells. *Nucleic Acids Res* 2020; **48**: W509-W514 [PMID: 32442275 DOI: 10.1093/nar/gkaa407]

18 **Ru B**, Wong CN, Tong Y, Zhong JY, Zhong SSW, Wu WC, Chu KC, Wong CY, Lau CY, Chen I, Chan NW, Zhang J. TISIDB: an integrated repository portal for tumor-immune system interactions. *Bioinformatics* 2019; **35**: 4200-4202 [PMID: 30903160 DOI: 10.1093/bioinformatics/btz210]

19 **Robin X**, Turck N, Hainard A, Tiberti N, Lisacek F, Sanchez JC, Müller M. pROC: an open-source package for R and S+ to analyze and compare ROC curves. *BMC Bioinformatics* 2011; **12**: 77 [PMID: 21414208 DOI: 10.1186/1471-2105-12-77]

20 **Asplund A**, Edqvist PH, Schwenk JM, Pontén F. Antibodies for profiling the human proteome-The Human Protein Atlas as a resource for cancer research. *Proteomics* 2012; **12**: 2067-2077 [PMID: 22623277 DOI: 10.1002/pmic.201100504]

21 **Vasaikar SV**, Straub P, Wang J, Zhang B. LinkedOmics: analyzing multi-omics data within and across 32 cancer types. *Nucleic Acids Res* 2018; **46**: D956-D963 [PMID: 29136207 DOI: 10.1093/nar/gkx1090]

22 **Warde-Farley D**, Donaldson SL, Comes O, Zuberi K, Badrawi R, Chao P, Franz M, Grouios C, Kazi F, Lopes CT, Maitland A, Mostafavi S, Montojo J, Shao Q, Wright G, Bader GD, Morris Q. The GeneMANIA prediction server: biological network integration for gene prioritization and predicting gene function. *Nucleic Acids Res* 2010; **38**: W214-W220 [PMID: 20576703 DOI: 10.1093/nar/gkq537]

23 **Yu G**, Wang LG, Han Y, He QY. clusterProfiler: an R package for comparing biological themes among gene clusters. *OMICS* 2012; **16**: 284-287 [PMID: 22455463 DOI: 10.1089/omi.2011.0118]

24 **Li T**, Fan J, Wang B, Traugh N, Chen Q, Liu JS, Li B, Liu XS. TIMER: A Web Server for Comprehensive Analysis of Tumor-Infiltrating Immune Cells. *Cancer Res* 2017; **77**: e108-e110 [PMID: 29092952 DOI: 10.1158/0008-5472.CAN-17-0307]

25 **Yoshihara K**, Shahmoradgoli M, Martínez E, Vegesna R, Kim H, Torres-Garcia W, Treviño V, Shen H, Laird PW, Levine DA, Carter SL, Getz G, Stemke-Hale K, Mills GB, Verhaak RG. Inferring tumour purity and stromal and immune cell admixture from expression data. *Nat Commun* 2013; **4**: 2612 [PMID: 24113773 DOI: 10.1038/ncomms3612]

26 **Newman AM**, Liu CL, Green MR, Gentles AJ, Feng W, Xu Y, Hoang CD, Diehn M, Alizadeh AA. Robust enumeration of

cell subsets from tissue expression profiles. *Nat Methods* 2015; **12**: 453-457 [PMID: 25822800 DOI: 10.1038/nmeth.3337]

27 **Bindea G**, Mlecnik B, Tosolini M, Kirilovsky A, Waldner M, Obenauf AC, Angell H, Fredriksen T, Lafontaine L, Berger A, Bruneval P, Fridman WH, Becker C, Pagès F, Speicher MR, Trajanoski Z, Galon J. Spatiotemporal dynamics of intratumoral immune cells reveal the immune landscape in human cancer. *Immunity* 2013; **39**: 782-795 [PMID: 24138885 DOI: 10.1016/j.immuni.2013.10.003]

28 **Hänzelmann S**, Castelo R, Guinney J. GSVA: gene set variation analysis for microarray and RNA-seq data. *BMC Bioinformatics* 2013; **14**: 7 [PMID: 23323831 DOI: 10.1186/1471-2105-14-7]

29 **Langfelder P**, Horvath S. WGCNA: an R package for weighted correlation network analysis. *BMC Bioinformatics* 2008; **9**: 559 [PMID: 19114008 DOI: 10.1186/1471-2105-9-559]

30 **Szklarczyk D**, Gable AL, Nastou KC, Lyon D, Kirsch R, Pyysalo S, Doncheva NT, Legeay M, Fang T, Bork P, Jensen LJ, von Mering C. The STRING database in 2021: customizable protein-protein networks, and functional characterization of user-uploaded gene/measurement sets. *Nucleic Acids Res* 2021; **49**: D605-D612 [PMID: 33237311 DOI: 10.1093/nar/gkaa1074]

31 **Viallard C**, Larrivée B. Tumor angiogenesis and vascular normalization: alternative therapeutic targets. *Angiogenesis* 2017; **20**: 409-426 [PMID: 28660302 DOI: 10.1007/s10456-017-9562-9]

32 **Aoki M**, Fujishita T. Oncogenic Roles of the PI3K/AKT/mTOR Axis. *Curr Top Microbiol Immunol* 2017; **407**: 153-189 [PMID: 28550454 DOI: 10.1007/82_2017_6]

33 **Choi KY**, Kim JH, Park IS, Rho YS, Kwon GH, Lee DJ. Predictive gene signatures of nodal metastasis in papillary thyroid carcinoma. *Cancer Biomark* 2018; **22**: 35-42 [PMID: 29562496 DOI: 10.3233/CBM-170784]

34 **Pober JS**, Tellides G. Participation of blood vessel cells in human adaptive immune responses. *Trends Immunol* 2012; **33**: 49-57 [PMID: 22030237 DOI: 10.1016/j.it.2011.09.006]

35 **la Sala A**, Pontecorvo L, Agresta A, Rosano G, Stabile E. Regulation of collateral blood vessel development by the innate and adaptive immune system. *Trends Mol Med* 2012; **18**: 494-501 [PMID: 22818027 DOI: 10.1016/j.molmed.2012.06.007]

36 **Terrén I**, Orrantia A, Vitallé J, Zenarruzabeitia O, Borrego F. NK Cell Metabolism and Tumor Microenvironment. *Front Immunol* 2019; **10**: 2278 [PMID: 31616440 DOI: 10.3389/fimmu.2019.02278]

37 **St Paul M**, Ohashi PS. The Roles of CD8(+) T Cell Subsets in Antitumor Immunity. *Trends Cell Biol* 2020; **30**: 695-704 [PMID: 32624246 DOI: 10.1016/j.tcb.2020.06.003]

38 **Cui C**, Wang J, Fagerberg E, Chen PM, Connolly KA, Damo M, Cheung JF, Mao T, Askari AS, Chen S, Fitzgerald B, Foster GG, Eisenbarth SC, Zhao H, Craft J, Joshi NS. Neoantigen-driven B cell and CD4 T follicular helper cell collaboration promotes anti-tumor CD8 T cell responses. *Cell* 2021; **184**: 6101-6118.e13 [PMID: 34852236 DOI: 10.1016/j.cell.2021.11.007]

39 **Lamplugh Z**, Fan Y. Vascular Microenvironment, Tumor Immunity and Immunotherapy. *Front Immunol* 2021; **12**: 811485 [PMID: 34987525 DOI: 10.3389/fimmu.2021.811485]

40 **Chan TA**, Yarchoan M, Jaffee E, Swanton C, Quezada SA, Stenzinger A, Peters S. Development of tumor mutation burden as an immunotherapy biomarker: utility for the oncology clinic. *Ann Oncol* 2019; **30**: 44-56 [PMID: 30395155 DOI: 10.1093/annonc/mdy495]

41 **Cristescu R**, Mogg R, Ayers M, Albright A, Murphy E, Yearley J, Sher X, Liu XQ, Lu H, Nebozhyn M, Zhang C, Lunceford JK, Joe A, Cheng J, Webber AL, Ibrahim N, Plimack ER, Ott PA, Seiwert TY, Ribas A, McClanahan TK, Tomassini JE, Loboda A, Kaufman D. Pan-tumor genomic biomarkers for PD-1 checkpoint blockade-based immunotherapy. *Science* 2018; **362** [PMID: 30309915 DOI: 10.1126/science.aar3593]

42 **He L**, Zhou X, Qu C, Tang Y, Zhang Q, Hong J. Serglycin (SRGN) overexpression predicts poor prognosis in hepatocellular carcinoma patients. *Med Oncol* 2013; **30**: 707 [PMID: 23996242 DOI: 10.1007/s12032-013-0707-4]

43 **Xu Y**, Xu J, Yang Y, Zhu L, Li X, Zhao W. SRGN Promotes Colorectal Cancer Metastasis as a Critical Downstream Target of HIF-1α. *Cell Physiol Biochem* 2018; **48**: 2429-2440 [PMID: 30121667 DOI: 10.1159/000492657]

Published by **Baishideng Publishing Group Inc**
7041 Koll Center Parkway, Suite 160, Pleasanton, CA 94566, USA
Telephone: +1-925-3991568
E-mail: bpgoffice@wjgnet.com
Help Desk: https://www.f6publishing.com/helpdesk
https://www.wjgnet.com